In situ observation of austenite grain growth behavior in the simulated coarse-grained heat-affected zone of Ti-microalloyed steels

Xiang-liang Wan, Kai-ming Wu, Gang Huang, Ran Wei, and Lin Cheng

The State Key Laboratory of Refractories and Metallurgy, Hubei Collaborative Innovation Center for Advanced Steels, Wuhan University of Science and Technology, Wuhan 430081, China

Abstract: The austenite grain growth behavior in a simulated coarse-grained heat-affected zone during thermal cycling was investigated via *in situ* observation. Austenite grains nucleated at ferrite grain boundaries and then grew in different directions through movement of grain boundaries into the ferrite phase. Subsequently, the adjacent austenite grains impinged against each other during the $\alpha \rightarrow \gamma$ transformation. After the $\alpha \rightarrow \gamma$ transformation, austenite grains coarsened via the coalescence of small grains and via boundary migration between grains. The growth process of austenite grains was a continuous process during heating, isothermal holding, and cooling in simulated thermal cycling. Abundant finely dispersed nanoscale TiN particles in a steel specimen containing 0.012wt% Ti effectively retarded the grain boundary migration, which resulted in refined austenite grains. When the Ti concentration in the steel was increased, the number of TiN particles decreased and their size coarsened. The big particles were not effective in pinning the austenite grain boundary movement and resulted in coarse austenite grains.

Keywords: alloy steel; austenite; grain growth; heat-affected zone; coarsening; titanium nitride

1. Introduction

High-strength low-alloy (HSLA) steels are important structural materials. They have good mechanical properties, including high strength, resistance to brittle fracture, cold formability, and good weldability. When HSLA steels are welded with large heat input, the grains of the coarse-grained heat-affected zone (CGHAZ) are coarsened, and the mechanical properties deteriorate. The austenite grains grow via grain boundary migration [1], which can be inhibited by the presence of particles of a second phase, thereby producing a grain boundary pinning effect [2]. This grain growth inhibition has different effects, depending on the size and fraction of precipitates [3]. A large volume fraction of fine particles is most effective in inhibiting grain growth. Previous studies have shown that the existing austenite grains in the CGHAZ can be refined by the addition of Ti as the microalloying element [4–6]. The addition of a small amount of Ti can lead to the dispersion of small-sized nanoscale TiN precipitates and effectively inhibit the austenite grain growth

[7]. However, the level of Ti addition must be carefully controlled, otherwise TiN particles will be coarse and their density will be reduced such that the austenite grains in the CGHAZ are coarsened [7].

Austenite nucleation and growth are known to be important phenomena in steel and to occur at high temperatures. The changes in the microstructure at high temperatures cannot be observed. Furthermore, the commencement of phase transformation cannot be identified and the mechanism by which the grain migration is hindered cannot be monitored. In recent years, the *in situ* observation of changes in the microstructure at high temperatures has been demonstrated to be a useful approach to investigate the phase transformation, grain growth, and precipitation phenomena in steels [8–12].

In the present work, *in situ* observation was utilized to observe the austenite grain growth during high heat input welding thermal cycles. The objective of the present study was to investigate the austenite grain growth behavior in the simulated weld CGHAZ of Ti-microalloyed steels.

Corresponding author: Kai-ming Wu   E-mail: wukaiming@wust.edu.cn

Ⓐ Springer

2. Experimental

Three experimental steels microalloyed with different levels of Ti (0.012wt%, 0.040wt%, and 0.061wt%) were prepared in a 10-kg vacuum melt induction furnace. The chemical compositions of the steels are listed in Table 1. The ingots were forged into plates, machined into cylindrical specimens of 5 mm in diameter and 5 mm in length, and mounted in an alumina crucible of 0.5 mm in thickness. The *in situ* observation was conducted using a high-temperature laser scanning confocal microscope and an infrared image furnace. A thermocouple with a precision of 0.1°C was positioned under the crucible and used to measure the temperature in the furnace. The specimens were heated to 1350–1400°C at a rate of 5°C/s, maintained at 1350–1400°C for 5–30 s for austenitization, and then cooled at a rate of 5°C/s, as shown in Fig. 1. Photographs were taken at a rate of 1 image per second during the simulated thermal cycling to observe the growth behavior of austenite grains. The size of the austenite grains was measured using a mean linear intercept method. After the specimens were heat-treated, scanning electron microscopy (SEM) observations and energy-dispersive X-ray spectroscopy (EDS) analyses were conducted using an LEO1450 instrument and transmission electron microscopy (TEM) studies were performed by a Tecnai G2.20 microscope operated at 200 kV.

Table 1. Chemical composition of the investigated steels

wt%

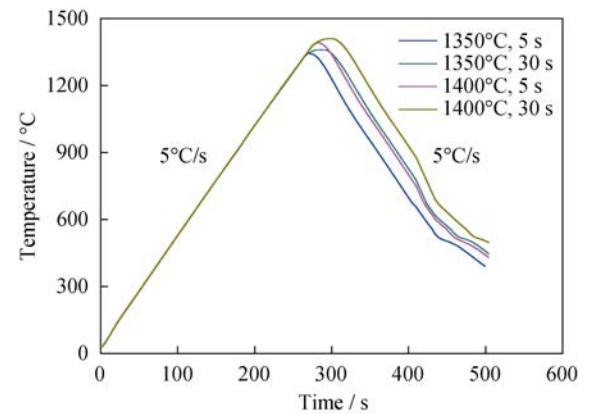| Sample	C	Si	Mn	Nb	Als	Ti	N	Ti/N
1#	0.055	0.22	1.61	0.022	0.051	0.012	0.0044	2.72
2#	0.058	0.21	1.60	0.025	0.055	0.040	0.0036	11.11
3#	0.057	0.23	1.63	0.023	0.057	0.061	0.0037	16.49

Fig. 1. Heat treatment patterns used for *in situ* observations.

3. Results

3.1. Grain growth behavior during α→γ transformation

Fig. 2 shows the *in situ* observations of the growth of austenite grains in the α-phase in 0.012wt% Ti steel during
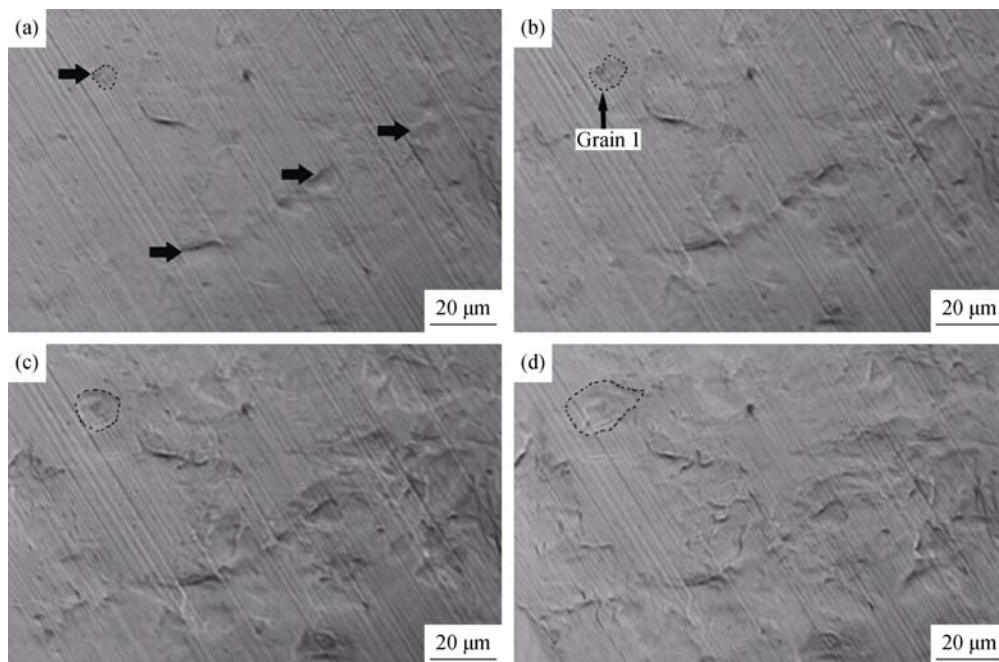

Fig. 2. *In situ* observation of the growth of austenite grains into the ferrite in the alloy containing 0.012wt% Ti at different temperatures: (a) 917.4°C; (b) 932.8°C; (c) 947.6°C; (d) 962.2°C. The arrows mark austenite grains; the dotted lines indicate grain boundaries.

heating. A few small austenite grains (indicated by arrows) nucleated on the surface of the specimen. Dotted lines in Fig. 2 represent the grain boundaries. Austenite grain 1 gradually extended outward in different directions with the increase in temperature, such that the grain grew into the α-phase by grain boundary movement. Fig. 3(a) shows the isolated small grains of austenite (grains 2–5) that separated from the α-phase in 0.012wt% Ti steel during the early stage of transformation. As the time progressed, the grains impinged against each other (Fig. 3(b)) and gradually covered the surface of the specimen (Fig. 3(c)).

3.2. Grain growth behavior in the γ-phase

After the α→γ transformation was completed, austenite grains continued to grow during the simulated thermal cycle. Figs. 4–6 show typical *in situ* images of the grain growth behavior in the γ-phase in 0.012wt% Ti steel at high temperatures (1250–1400°C). Notably, the small grains (grains 6–8) in Fig. 4(a) coalesced at 1311°C to form a large grain

(grain 9) and then grew into neighboring grains (as indicated by arrows in Fig. 4(a)) though grain boundary movement (Fig. 4(b)). Fig. 5 presents an example of the disappearance of a small austenite grain during the grain growth process. The small grain (grain 10) in Fig. 5(a) was swallowed by three neighboring austenite grains (grains 11–13) via emigration of the grain boundary during the isothermal holding period at 1400°C, as shown in Fig. 5(b). Fig. 6 shows that the grain boundary moved from position 1 to position 2. In a similar manner, the coalescence and disappearance of small grains and grain boundary movement were also observed in the other two steels with different Ti concentrations.

3.3. Measured grain size during thermal cycling

The size of austenite grains at different temperatures was measured from *in situ* images using a mean linear intercept method. Fig. 7 shows the change in the mean austenite grain size of three experimental steels microalloyed with different
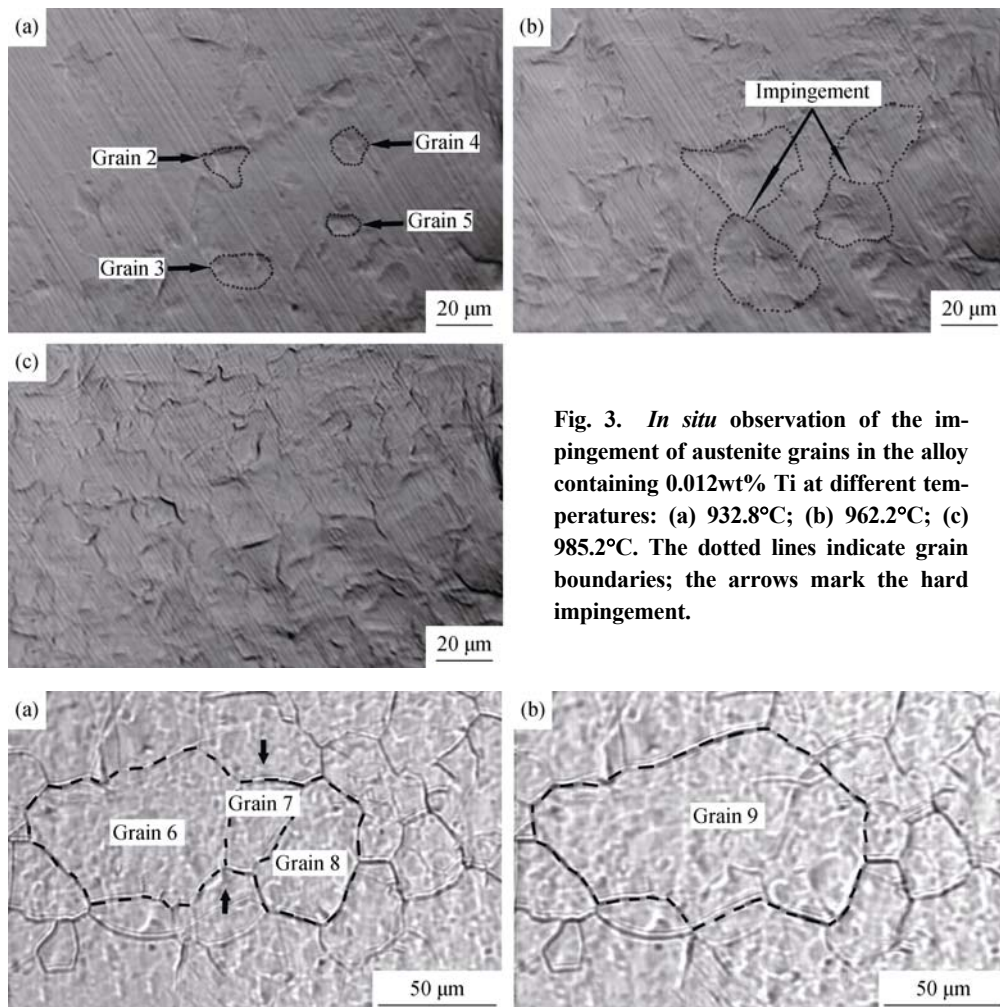

Fig. 3. *In situ* observation of the impingement of austenite grains in the alloy containing 0.012wt% Ti at different temperatures: (a) 932.8°C; (b) 962.2°C; (c) 985.2°C. The dotted lines indicate grain boundaries; the arrows mark the hard impingement.

Fig. 4. *In situ* observations of the coalescence of austenite grains in the alloy containing 0.012wt% Ti at different temperatures: (a) 1311.3°C; (b) 1350.8°C (grain 9 was formed by coalescence of grain 6–8).
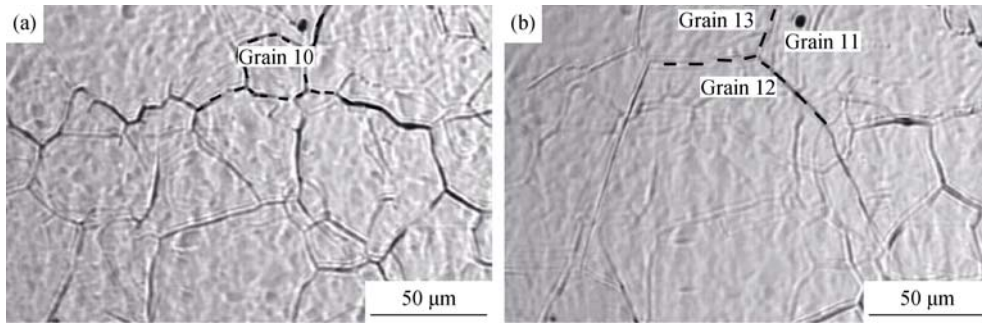
Fig. 5. *In situ* observations of the disappearance of small austenite grains in the alloy containing 0.012wt% Ti at different temperatures: (a) 1400.6°C; (b) 1398.4°C.
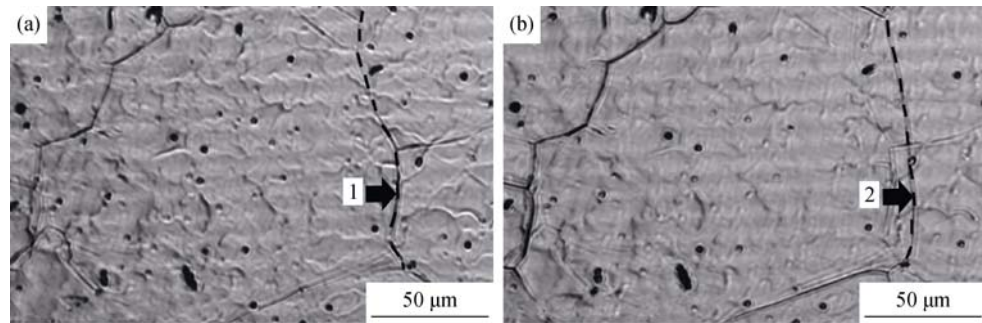

Fig. 6. *In situ* observations of the movement of grain boundaries of the austenite grains in the alloy containing 0.012wt% Ti at different temperatures: (a) 1358.0°C; (b) 1256.3°C.
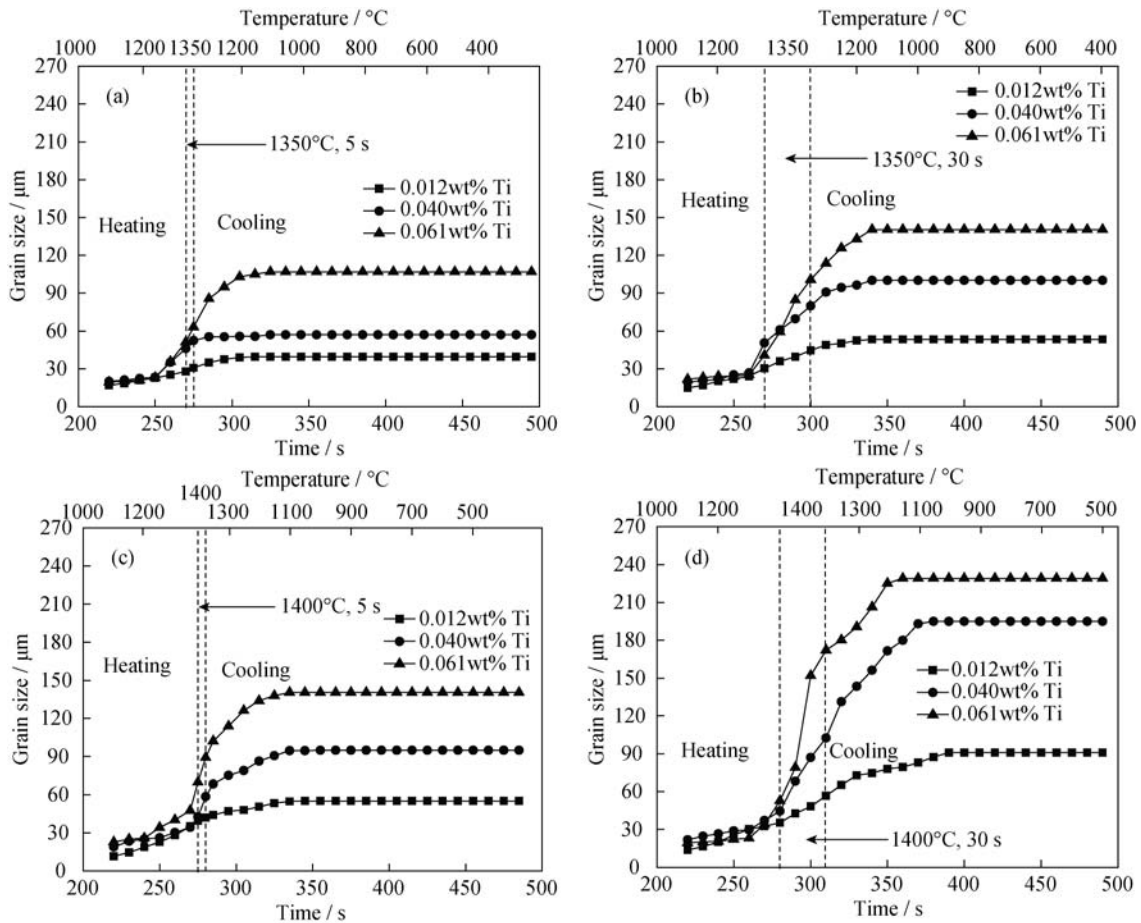

Fig. 7. Measured austenite grain size in the three experimental steels isothermally held at 1350°C for 5 s (a), 1350°C for 30 s (b), 1400°C for 5 s (c), and 1400°C for 30 s (d).

levels of Ti during thermal cycling with different peak temperatures and holding times. The austenite grain growth process was continuous. The grains grew continuously during heating, isothermal holding, and cooling. The growth of the austenite grains stopped during the cooling process when the temperature decreased to less than 1150°C. When the peak temperature was increased or the holding time was

prolonged, the austenite grains became larger. We also observed that the size of austenite grains was larger in the specimens with greater levels of Ti addition.

3.4. Particle analysis

Fig. 8 shows the typical morphologies of particles in the three specimens heated at 1400°C for 5 s. The size
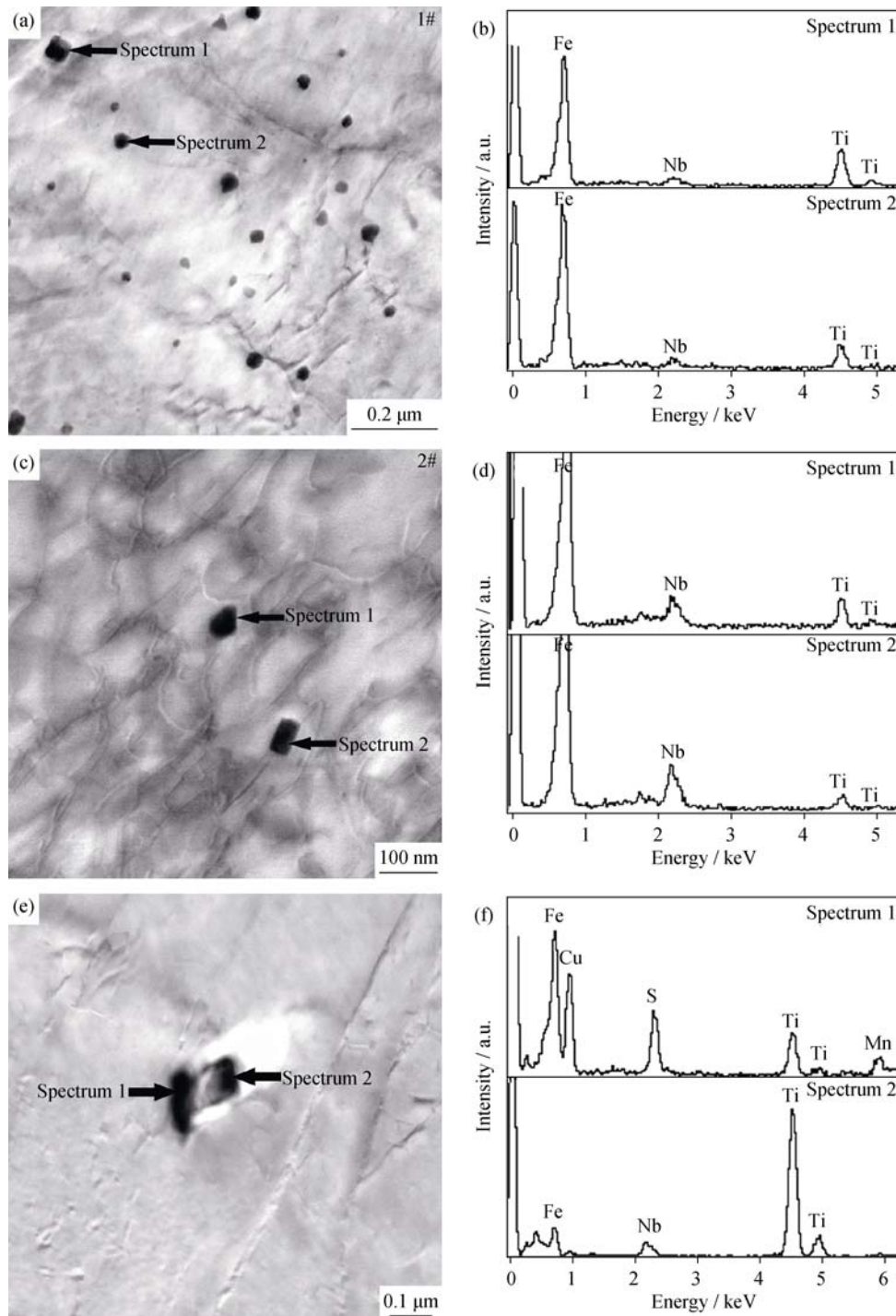

Fig. 8.   TEM micrographs and EDS analysis of precipitates in steels containing different concentrations of Ti: (a,b) 0.012wt%; (c,d) 0.040wt%; (e,f) 0.061wt%. Specimens were isothermally held at 1400°C for 5 s.

distribution of the particles for each specimen measured from 25 TEM micrographs is presented in Table 2. A large number of particles were observed in the steel contained 0.012wt% Ti (Fig. 8(a)), and the average equivalent diameter of the precipitates was 36 nm (Table 2). In the case of the steels contained 0.040wt% and 0.061wt% Ti (Figs. 8(c) and 8(e)), the number of particles was substantially decreased,

and the average equivalent diameter of particles was increased to 65 and 112 nm, respectively (Table 2), such that sub-micron and micrometer-sized particles were observed in the steel with 0.061wt% Ti. A typical SEM micrograph of a precipitate and its corresponding EDS analysis results are presented in Fig. 9. The sub-micron particle consisted of an aluminum oxide core and a titanium nitride shell.

Table 2.   Size distribution of nanoscale particles in the specimens held at 1400°C for 5 s

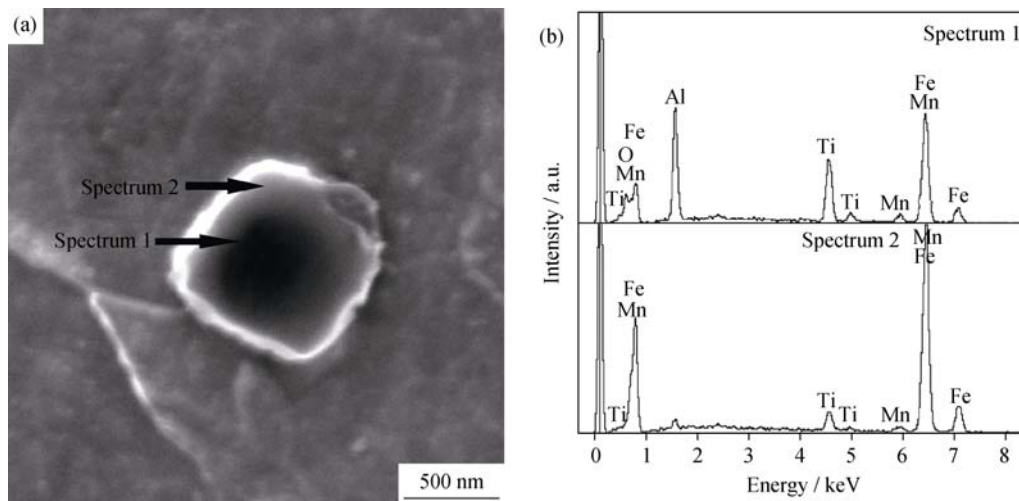| Concentration of Ti / wt%	Number of particles							Average diameter / nm
	Total number	0–30 nm	31–60 nm	61–90 nm	91–120 nm	121–150 nm	151–180 nm	181–210 nm	
0.012	351	143	175	29	4	0	0	0	36.3
0.040	90	2	44	34	6	2	2	0	64.7
0.061	29	0	3	4	12	3	6	1	112.5

Fig. 9.   SEM micrograph (a) and EDS spectra (b) of a precipitate in the steel containing 0.061wt% Ti. The specimen was isothermally held at 1400°C for 5 s.

4. Discussion

4.1. Austenite grain growth behavior at high temperatures

Numerous researchers have investigated the austenite grain growth behavior using isothermal treatments [13], *in situ* measurements [14], and simulated mode predictions [15]. Their results indicate that austenite grains grow by boundary movement and are affected by secondary precipitates [2]. Austenite grains grow quickly at high temperatures and become large with the increase in peak temperature [16].

In the present work, the *in situ* micrographs indicated that austenite grains nucleated at the α-phase boundary and gradually extended outward in different directions by grain boundary migration. A similar behavior was observed by *in situ* observation of cyclic partial phase transformations [17]. With the continuation of α→γ transformation, more small grains nucleated, and grain growth occurred via the im-

pingement of grains until the transformation was complete. After the α→γ transformation, the microstructure of the specimens consisted of austenite grains. At high temperatures, small austenite grains competed for growth; some of them coalesced and formed large grains. The boundaries of these large grains moved, resulting in small neighboring grains being "swallowed."

The austenite grain growth process is a continuous process (Fig. 7). They grew during the heating, isothermal holding, and cooling processes. During high-temperature processes, grains grew rapidly because of the dissolution of particles and an ineffectual pinning effect [18]. A comparison of final grain sizes reached at different peak temperatures and different holding times revealed that austenite grains became large as the peak temperature and holding time increased. The grain growth stopped when the temperature decreased to less than 1150°C during the cooling process (Fig. 7).

4.2. Pinning effect of nanoscale TiN particles on the austenite grain growth

The grain boundary migration is well known to be influenced by the presence of second-phase particles [2]. The particle diameter and volume fraction influence the austenite grain size, and the size and fraction of particles can change during thermal cycling [18]. TiN is precipitated at high temperatures when the product of the total Ti and N concentrations is greater than the solubility product of TiN [5]. Solidification is the most significant process for the formation of coarse TiN particles [19]. Hence, control of the total Ti and N levels is necessary to ensure that the product of the concentrations is less than the solubility product at the solidus.

The solubility product for TiN in austenite is given by Eq. (1) [17,20]:

$$\lg\left\{[\text{Ti}_{\text{dissolved}}][\text{N}_{\text{dissolved}}]\right\}_{\gamma} = 4.35 - 14890\big/T \tag{1}$$

where $[\text{Ti}_{\text{dissolved}}]$ and $[\text{N}_{\text{dissolved}}]$ are the concentrations of Ti and N dissolved in the austenite phase, respectively, and T is the absolute temperature. Control of the ratio between Ti and N concentrations is also important because this ratio

should match the stoichiometric value of 3.42; that is

$$\frac{[\text{Ti}_{\text{total}}] - [\text{Ti}_{\text{dissolved}}]}{[\text{N}_{\text{total}}] - [\text{N}_{\text{dissolved}}]} = 3.42 \tag{2}$$

where $[\text{Ti}_{\text{total}}]$ and $[\text{N}_{\text{total}}]$ are the Ti and N concentrations in the steel, respectively. By combining Eqs. (1) and (2), we calculated the precipitated TiN for the three steels investigated in this work, as shown in Fig. 10(a). The solidification temperature (1521°C) for these steels was calculated using the Thermo-calc software in conjunction with the SSOL4 database. The results reveal that TiN particles will precipitate after solidification in the steel containing 0.012wt% Ti such that TiN will be small and disperses in the matrix. However, the products of the total Ti and N concentrations in the steels with 0.040wt% and 0.061wt% Ti are 1.44 × 10^{-4} and 2.26 × 10^{-4}, respectively. They are greater than the solubility product (1.12 × 10^{-4}) at the solidification temperature (Fig. 10(a)). TiN particles will precipitate before solidification. Thus, they were already coarsened at high temperatures before solidification. Meanwhile, the mass fraction of TiN particles (Fig. 10(a)) was almost unchanged when the temperature was less than 1150°C.
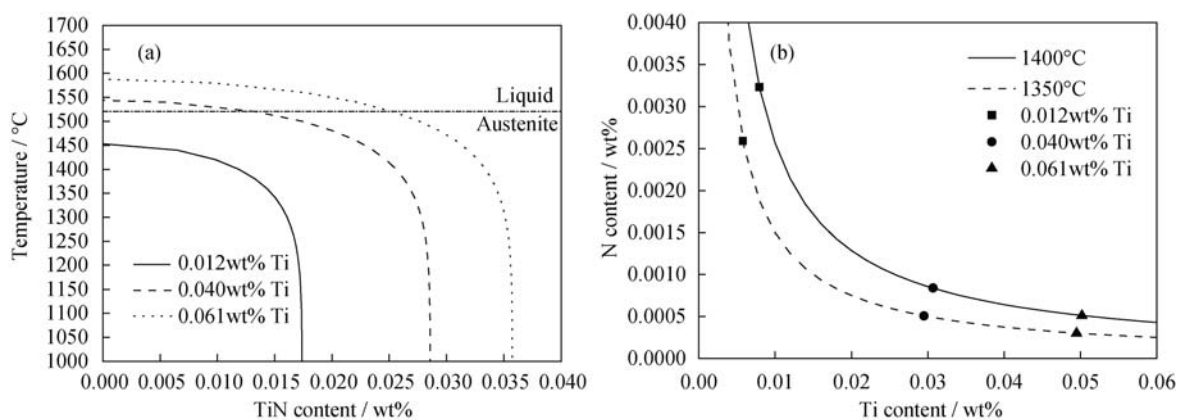

Fig. 10. Curves of the content of TiN particles varying with temperature (a) and the concentrations of dissolved Ti and N in austenite at different peak temperatures (b).

TiN particles in the CGHAZ were partially dissolved during thermal cycling. The concentrations of dissolved Ti and N are important with respect to the coarsening of TiN [19]. Fig. 10(b) shows the concentrations of dissolved Ti and N at the peak temperature. A larger concentration of dissolved Ti and a smaller concentration of dissolved N were present in the steels contained 0.040wt% and 0.061wt% Ti. The ratio of $[\text{Ti}_{\text{dissolved}}]$ to $[\text{N}_{\text{dissolved}}]$ was greater than 3.42, except in the steel contained 0.012wt% Ti. Thus, the greater concentration of dissolved Ti in the steels containing 0.040wt% and 0.061wt% Ti promoted coarsening of TiN during the cooling process [20], as demonstrated

in the TEM micrographs (Fig. 8 and Table 2). The austenite grain size increased as the amount of Ti added was increased (Fig. 7 and Table 2).

5. Conclusions

(1) During the α→γ transformation, austenite grains nucleated at ferrite grain boundaries and grew in different directions through grain boundary migration into the ferrite, followed by impingement of austenite grains against each other.

(2) After the α→γ transformation, small austenite grains

competed for growth; some of them coalesced and formed large grains. The boundaries of large grains moved, which resulted in large grains swallowing small neighboring grains.

(3) The austenite grain growth was a continuous process during heating, isothermal holding, and cooling in the simulated thermal cycling. The growth of austenite grains stopped during cooling when the temperature decreased to less than 1150°C.

(4) When the Ti concentration was small, a large number of nanoscale TiN particles formed and dispersed into the steel matrix, which effectively inhibited the growth of austenite grains. However, greater Ti concentrations led to coarsening of austenite grains because the low density of coarse particles was ineffective in pinning the movement of the grains.

Acknowledgements

References

[1]   K.L. Merkle, L.J. Thompson, and F. Phillipp, *In-situ* HREM studies of grain boundary migration, *Interface Sci.*, 12(2004), No. 2-3, p. 277.

[2]   M. Sugiyama and G. Shigesato, Development of in situ microstructure observation technique in steel, *Nippon Steel Tech. Rep.*, 91(2005), p. 13.

[3]   P.A. Manohar, M. Ferry, and T. Chandra, Five decades of the Zener equation, *ISIJ Int.*, 38(1998), No. 9, p. 913.

[4]   M. Sasaki, K. Matsuura, K. Ohsasa, and M. Ohno, Effects of addition of titanium and boron on columnar austenite grain in carbon steel, *ISIJ Int.*, 49(2009), No. 9, p. 1367.

[5]   T.N. Baker, *Titanium Technology in Microalloyed Steels*, 2nd Ed., The Institute of Materials, Minerals and Mining, London, 1997.

[6]   T. Gladman, *The Physical Metallurgy of Microalloyed Steels*, The Institute of Materials, Minerals and Mining, London, 1997.

[7]   W. Yan, Y.Y. Shan, and K. Yang, Effect of TiN inclusions on the impact toughness of low-carbon microalloyed steels, *Metall. Mater. Trans. A*, 37(2006), No. 7, p. 2147.

[8]   D. Zhang, H. Terasaki, and Y. Komizo, *In situ* observation of the formation of intragranular acicular ferrite at non-metallic inclusions in C–Mn steel, *Acta Mater.,* 58(2010), No. 4, p. 1369.

[9]   D. Phelan, N. Stanford, and R. Dippenaar, *In situ* observations of Widmanstätten ferrite formation in a low-carbon steel, *Mater. Sci. Eng. A,* 407(2005), No. 1-2, p. 127.

[10]   S.E. Offerman, N.H. van Dijk, J. Sietsma, S. Grigull, E.M. Lauridsen, L. Margulies, H.F. Poulsen, M.Th. Rekveldt, and V. van der Zwaag, Grain nucleation and growth during phase transformations, *Science,* 298(2002), No. 5595, p. 1003.

[11]   X.J. Shao, X.H. Wang, W.J. Wang, F.X. Huang, and M. Jiang, *In-situ* observation of manganese sulfide inclusions in YF45MnV steel, *J. Univ. Sci. Technol. Beijing,* 32(2010), No. 5, p. 570.

[12]   X.L. Wan, R. Wei, L. Cheng, M. Enomoto, and Y. Adachi, Lengthening kinetics of ferrite plates in high-strength low-carbon low alloy steel, *J. Mater. Sci.,* 48(2013), No. 12, p. 4345.

[13]   Q.B. Yu and Y. Sun, Abnormal growth of austenite grain of low-carbon steel, *Mater. Sci. Eng. A,* 420(2006), No. 1-2, p. 34.

[14]   M. Maalekian, R. Radis, M. Militzer, A. Moreau, and W.J. Poole, *In situ* measurement and modelling of austenite grain growth in a Ti/Nb microalloyed steel, *Acta Mater.,* 60(2012), No. 3, p. 1015.

[15]   J. Moon, J. Lee, and C. Lee, Prediction for the austenite grain size in the presence of growing particles in the weld HAZ of Ti-microalloyed steel, *Mater. Sci. Eng. A,* 459(2007), No. 1-2, p. 40.

[16]   S.S. Zhang, M.Q. Li, Y.G. Liu, J. Luo, and T.Q. Liu, The growth behavior of austenite grain in the heating process of 300M steel, *Mater. Sci. Eng. A,* 528(2011), No. 15, p. 4967.

[17]   H. Chen, E. Gamsjäger, S. Schider, H. Khanbareh, and S. van der Zwaag, *In situ* observation of austenite-ferrite interface migration in a lean Mn steel during cyclic partial phase transformations, *Acta Mater.,* 61(2013), No. 7, p. 2414.

[18]   J. Moon, C. Lee, S. Uhm, and J. Lee, Coarsening kinetics of TiN particle in a low alloyed steel in weld HAZ: considering critical particle size, *Acta Mater.,* 54(2006), No. 4, p. 1053.

[19]   M.T. Nagata, J.G. Speer, and D.K. Matlock, Titanium nitride precipitation behavior in thin-slab cast high-strength low-alloy steels, *Metall. Mater. Trans. A,* 33(2002), No. 10, p. 3099.

[20]   K. Inoue, I. Ohnuma, H. Ohtani, K. Ishida, and T. Nishizawa, Solubility product of TiN in austenite, *ISIJ Int.,* 38(1998), No. 9, p. 991.